



Published in final edited form as:

Technol Cancer Res Treat. 2015 June ; 14(3): 298–304. doi:10.1177/1533034614547447.

Qualitative Evaluation of Fiducial Markers for Radiotherapy Imaging

Maria F. Chan, PhD¹, Gil'ad N. Cohen, MS¹, and Joseph O. Deasy, PhD¹

¹Department of Medical Physics, Memorial Sloan-Kettering Cancer Center, New York, NY, USA

Abstract

Purpose—To evaluate visibility, artifacts, and distortions of various commercial markers in magnetic resonance imaging (MRI), computer tomography (CT), and ultrasound imaging used for radiotherapy planning and treatment guidance.

Methods—We compare 2 solid gold markers, 4 gold coils, and 1 polymer marker from 3 vendors. Imaging modalities used were 3-T and 1.5-T GE MRIs, Siemens Sequoia 512 Ultrasound, Phillips Big Bore CT, Varian Trilogy linear accelerator (cone-beam CT [CBCT], on-board imager kilovoltage [OBI-kV], electronic portal imaging device megavoltage [EPID-MV]), and Medtronic O-ARM CBCT. Markers were imaged in a $30 \times 30 \times 10$ cm³ custom bolus phantom. In one experiment, Surgilube was used around the markers to reduce air gaps. Images were saved in Digital Imaging and Communications in Medicine (DICOM) format and analyzed using an in-house software. Profiles across the markers were used for objective comparison of the markers' signals. The visibility and artifacts/distortions produced by each marker were assessed qualitatively and quantitatively.

Results—All markers are visible in CT, CBCT, OBI-kV, and ultrasound. Gold markers below 0.75 mm in diameter are not visible in EPID-MV images. The larger the markers, the more CT and CBCT image artifacts there are, yet the degree of the artifact depends on scan parameters and the scanner itself. Visibility of gold coils of 0.75 mm diameter or larger is comparable across all imaging modalities studied. The polymer marker causes minimal artifacts in CT and CBCT but has poor visibility in EPID-MV. Gold coils of 0.5 mm exhibit poor visibility in MRI and EPID-MV due to their small size. Gold markers are more visible in 3-T T1 gradient-recalled echo than in 1.5-T T1 fast spin-echo, depending on the scan sequence. In this study, all markers are clearly visible on ultrasound.

Conclusion—All gold markers are visible in CT, CBCT, kV, and ultrasound; however, only the large diameter markers are visible in MV. When MR and EPID-MV imagers are used, the selection of fiducial markers is not straightforward. For hybrid kV/MV image-guided radiotherapy imaging, larger diameter markers are suggested. If using kV imaging alone, smaller sized markers

Reprints and permission: sagepub.com/journalsPermissions.nav

Corresponding Author: Maria F. Chan, PhD, Department of Medical Physics, Memorial Sloan-Kettering Cancer Center, 1275 York Avenue, New York, NY 10065, USA. chanm@mskcc.org.

Declaration of Conflicting Interests

The author(s) declared no potential conflicts of interest with respect to the research, authorship, and/or publication of this article.

may be used in smaller sized patients in order to reduce artifacts. Only larger diameter gold markers are visible across all imaging modalities.

Keywords

radiotherapy; fiducial markers; target motion; IGRT

Introduction

Fiducial markers are used in a wide range of medical imaging applications. Images of the same patient produced with 2 different imaging systems may be correlated by placing fiducial markers in the area imaged by both the systems. For example, functional information from single-photon emission computed tomography or positron emission tomography can be related to anatomical information provided by magnetic resonance imaging (MRI).¹ Similarly, fiducial points established during MRI can be correlated with brain images generated by magnetoencephalography (MEG) to localize the source of brain activity. The locations of the fiducial points in each data set are then used to define a common coordinate system, so that superimposing the functional MEG data onto the structural MRI data is possible.² Fiducial markers have also been used in radiotherapy to assist with the registration process³⁻⁶ due to the inter- and intrafractional target motion observed in radiation treatments for various cancer sites.^{3,7-9}

Multimodality imaging including magnetic resonance (MR) and computer tomography (CT) simulations and image-guided radiotherapy (IGRT) has been used in the radiation treatment of patients with cancer. Different IGRT techniques include, but are not limited to ultrasound,^{5,10} linear accelerator (Linac)-based kilovoltage (kV)/megavoltage (MV) x-rays,^{3-6,11,12} in-room CT on rail, and kV or MV cone-beam CT (CBCT).^{6,13} Ultrasound IGRT is typically based on soft tissue anatomy, not directly involving fiducial markers for guidance. However, in many institutions, clinicians implant fiducial markers during prostate brachytherapy for guiding conformal external beam radiation therapy.⁵ As for x-ray-based IGRT systems, fiducial markers are used to assist with registration, tracking interfraction/intrafraction tumor motion, and measuring positioning differences from the process of simulation to treatment planning to treatment guidance. Daily localization from Linac-based kV/MV orthogonal fiducial imaging has become routine for prostate cancer in many radiotherapy clinics due to its requirement of less physician input and time saving when compared to CBCT.⁶

Fiducial markers are commonly placed inside or adjacent to the target volumes prior to radiotherapy simulation and serve as surrogates to the target volumes. Ideally, the fiducial markers should be easily identified and clearly visible on both simulation and treatment verification images. The utilization of the fiducial markers in pretreatment image registration can assist therapists/clinicians to objectively align the target volumes, thereby treating the tumors precisely and sparing the surrounding normal tissues. Difficulty arises when artifacts from the fiducial markers obscure a small tumor completely, especially in tumors with low tumor to parenchyma contrast,¹⁴ and the artifacts affect the clarity of the anatomical region of interest. As MR simulators have emerged, we have to reevaluate

among available markers those that perform optimally for hybrid MR/CT imaging during simulation as well as treatment. Most of the published reports on the evaluation of fiducial markers for IGRT did not include MR imaging (MRI) in their comparison,^{15,16} although there have been studies on the artifacts of fiducial markers in MRI.^{17,18} Although there are many commercially available markers, the choice may not be obvious. Our aim is to provide practical guidance to clinicians in selecting optimal fiducial markers for image-guided radiotherapy. To do this, we evaluated 7 commercially available markers across a variety of imaging modalities including 2 different strengths of MR scanners (a total of 8 imaging devices) used throughout the IGRT process.

Materials and Methods

Imaging equipment used in this study included 2 MR scanners with 2 different magnetic strengths (GE 1.5-T MR Scanner and Philips 3-T MR Simulator), a Philips Big Bore Brilliance CT scanner (120 kVp), a Siemens ultrasound unit, Varian Trilogy imaging options CBCT (125 kVp), OBI-kV (80 kVp, 200 mA), and electronic portal imaging device (EPID) MV imagers (6 MV), and a Medtronic O-Arm CBCT (140 kVp) which, at our institution, is used intraoperatively for brachytherapy procedures. The parameter settings used in MRI were those typically used for a prostate protocol/sequence. For example, T1-fast spin-echo (FSE), 35 cm field of view (FOV), repetition time (TR)/echo time (TE) 483/8 ms, 2 NEX, and T1-gradient-recalled echo (GRE), 40 cm FOV, TR/TE 5/3 ms, 4 NEX, for 1.5-T and 3-T MRI, respectively. Seven fiducial markers were evaluated from 3 vendors: VisiCoil (IBA, Radiomed Group, Bartlett, TN), Solid Gold (Alpha-Omega Services, Bellflower, CA), and FusionCoil and PolyMark (CIVCO Medical Solution, Orange City, IA). The physical dimensions of the markers are shown in Figure 1. We evaluated the markers according to their potential usability in our standard workflow of patient treatment both in external beam and in brachytherapy services at the Memorial Sloan-Kettering Cancer Center.

All markers were placed in a $30 \times 30 \times 10$ cm³ custom bolus phantom (Radiation Products Design, Albertville, MN) and imaged together in all imaging devices. In one experiment, Surgilube™ (Savage Laboratories, Melville, NY, USA) was used around the markers to reduce air gaps. We tried to scan the phantom using the same or similar imaging parameters (spacing, thickness, and FOV), such as 2- to 3-mm slice thickness, depending on the availability of that setting in the scanner employed. The monitor unit setting used was 1 and 2 MU for the EPID-MV images. All images were saved in Digital Imaging and Communications in Medicine (DICOM) format and analyzed using in-house software (Overlay). Profiles across the markers were used for objective comparison of the markers' signals. The visibility and artifacts/distortions produced by each marker were assessed qualitatively and quantitatively. Note that the bolus phantom is of a specific size and uniform density, and thus, the visibility of markers under MRI might not be the best representation of that in the real-world imaging of human anatomy.

We have also tested some markers with extra coating material in order to see whether the gold markers would be brightened in MR images. Those markers were coated with a thin layer of polymer-based material (i.e. maleic anhydride) using a particle size analyzer in a

chemical laboratory. The chemical composition of the coating can be evaluated using the analysis of particle distribution software.

Results and Discussion

Figure 1 shows the table of the cropped images of the markers for each modality. As can be seen, all gold markers are visible in CT, CBCT, kV, and ultrasound, yet only the large diameter markers are visible in MV. The markers in MR T1 images appear as a dark circle. Obviously, there are artifacts and distortions in the MR modalities since the image size is different than the physical size. Also note the streak artifacts from the gold markers both in CT and in CBCT images.

Figure 2A shows the bolus phantom—30 cm² and 10 cm high. Figure 2B shows the EPID-MV image of the 2 larger gold markers with and without coating. Figure 2C shows the Linac-based kV-CBCT image of 4 different sizes of VisiCoil markers. The visibility and artifacts/distortions produced by each marker were measured qualitatively and quantitatively using the profiling tool available in our in-house software. For example, Figure 2D shows the horizontal profile of a gold marker in the MR T1 image. As can be seen, the intensity of this marker in MR T1 is lower than the intensities across the horizontal profile. Figure 2E shows the horizontal profile across 5 markers in a row in a CT image. The signal intensity of the marker on the profile reflects the brightness in CT image. We also CT scanned the markers in different CT parameters. Figure 2F shows the comparison of 2 markers (solid gold and PolyMark) using 2 different scanning parameters in CBCT. As expected, scanning technique (kV mA setting) will impact the marker's visibility and artifacts.

Our study has shown that all markers are visible in CT, CBCT, OBI-kV, and ultrasound. Gold markers below 0.75 mm in diameter are not or are hardly visible in EPID-MV images. The larger the markers, the more the CT and CBCT image artifacts, yet the degree of the artifact depends on scan parameters. Visibility of gold coils of 0.75 mm diameter or larger is comparable across all imaging modalities studied. The polymer marker causes minimal artifacts in CT and CBCT but has poor visibility in EPID-MV. Gold coils of 0.5 mm exhibit poor visibility in MRI and EPID-MV due to their small size. Gold markers are more visible in 3-T T1-GRE than in 1.5-T T1-FSE, depending on the scan sequence. All markers in this study are clearly visible on ultrasound.

Our study has also shown that VisiCoil and FusionCoil are comparable. When MR and EPID-MV imagers are used, larger diameter markers are suggested. Whereas, when using kV imaging alone, smaller sized gold markers or polymer markers may be used in order to reduce artifacts. Attention should be paid to CT scan protocols and MR sequences in order to reduce image artifacts and ensure visibility of the markers. Further, clinical requirements, such as selection between T2 and T1, or use of contrast, must be considered and will vary with treatment site.

In addition to the commercially available markers, we have also compared the VisiCoil, FusionCoil, and PolyMark with some other “research and development” markers with MR, Linac-based MV/kV, and CBCT imaging using the 10-cm thick bolus phantom. Figure 3

shows the MR T1 axial images of the markers and Figure 4 shows the Linac-based OBI-kV, EPID-MV, and CBCT images of the markers. Again, to be visible in MV images, the marker size needs to be more than 0.75 mm in diameter. Therefore, for hybrid kV/MV IGRT, one should select at least a 0.75-mm diameter marker; however, if for kV images alone and/or with CBCT, one may select 0.5-mm diameter markers for less image artifacts.

An additional finding of this study was that the Surgilube gel (normally used in ultrasound imaging) will brighten up in MR T2 (T2-FSE, 35 cm FOV, TR/TE 4566/118 ms, 4 NEX) images and cause local artifacts. Therefore, we should avoid using the gel in MR T2 imaging.

Handsfield et al¹⁵ evaluated the visibility and artifacts created by gold, carbon, and polymer fiducial markers across CT, Linac-based kV/MV, and tomotherapy. They suggested polymer and carbon markers for target localization and patient treatment verification for kV imaging-based treatment because of less image artifacts and to use gold markers for position verification for MV imaging, despite the artifacts created on the simulation CT images. They reported that further studies are needed when mixed kV- and MV-based imaging schemes are used in a clinic. In our work, we have extended our studies to cover 2 different strengths of MR scanners (1.5T and 3T), hybrid kV/MV imaging modalities, and 2 different types of CBCT (Linac-based used in the radiation treatment room and O-Arm used in the intraoperative suite). Chen et al¹⁹ investigated a variety of commercially available fiducial markers implantable into the prostate for target localization and patient repositioning verification in an on-board kV imaging system on a proton gantry. The ratio of contrast to noise ratio to patient entrance skin exposure was introduced to characterize the efficiency for imaging a marker using a given x-ray technique in order to optimize the marker's visibility and simultaneously minimize the x-ray imaging dose. The authors suggested that markers should have a thickness greater than the equivalent of 0.14-mm thick gold in order to produce the acceptable visibility in the lateral kV imaging.

Habermehl et al¹⁶ also evaluated 5 different fiducial markers for IGRT and particle therapy. They reported that disturbances due to artifacts and dose perturbation were highest in the arbitrarily folded gold and the thickest gold marker but especially low in the carbon marker. Zhang et al²⁰ also investigated the dose perturbations introduced by the implanted gold fiducial markers in prostate cancer intensity-modulated proton therapy (IMPT) and the impacts of different plan designs on the perturbations. Their results showed that dose perturbation effects decreased with the increase in number of beam angles. Up to 6 beam angles may be required to reduce the dose perturbations from the gold fiducial markers to a clinically acceptable level in IMPT. Huang et al²¹ evaluated 12 fiducial markers for their potential clinical utility in proton radiation therapy for prostate cancer with the use of a CT and kV imaging system. The dose perturbation caused by each fiducial marker was quantified using radiochromic film and a clinical proton beam. Based on their analysis, 3 prototype fiducial markers were identified as good candidates for use in proton radiotherapy of prostate cancer. Cheung et al.²² reported that carbon-coated and stainless steel fiducials could be used in proton therapy if they are located far from the end of the range of the beam and if they are orientated perpendicular to the beam axis.

Jonsson et al¹⁷ studied the cylindrical gold markers and susceptibility effects in MRI simulation and measurement of spatial accuracy. They found that the depiction of the markers in MRI is dependent on their shape and orientation relative to the main magnetic field due to susceptibility effects. Their measurements revealed small position deviations (<1 mm) of the imaged marker positions relative to the actual marker positions. Huisman et al²³ prospectively compared the landmark and iterative closest point methods for registration of CT and MR images of the prostate gland after placement of fiducial markers. The authors found that precision of the iterative closest point method (1.1 mm) was significantly better ($P < .01$) than that of the landmark method (2.0 mm).

DeLangen et al²⁴ also investigated a large number of commercial fiducial markers including solid gold, gold coil, and polymer types in CT, x-ray, MRI, EPID, and ultrasound. They also found that all markers were visible in ultrasound. Solid markers were preferred in EPID. The best marker for x-rays was the result of an optimization between visibility in kV and minimization of CT distortion. For MRI, a marker should either have larger dimensions or contain a very small amount of steel. Henry et al²⁵ assessed the optimal marker length and diameter to be used with EPID on an 8 MV Elekta SL20 Linac. They found that markers less than 5 mm in length or 0.9 mm in diameter were poorly visualized (<70% visualization success in lateral EPID). The marker measuring 0.9 mm × 5 mm appears to be clinically optimal in pelvic radiotherapy patients (80% visualization success in lateral EPID) and will be used for actual organ implantation.

In our study, there are some nonuniformities or air gaps within the customized bolus phantom, and these may introduce some additional undesired artifacts. In a future study, we will focus on testing the effect of various sequences and sequencing parameters in MRI, therefore quantifying the distortion in anatomical and functional MRI, especially diffusion sequences by generating field maps from each marker. We are currently constructing a uniform MR/CT gel phantom consisting of agarose gel for this purpose. Also, the quantitative analysis will be conducted by computer software automatically instead of manually.

Conclusions

We have compared commercially available fiducial markers in various treatment imaging modalities and provided useful information for clinicians to choose optimal markers and imaging techniques. All gold markers are visible in CT, CBCT, kV, and ultrasound, yet only the large diameter markers are visible in MV. When MR and EPID-MV imagers are used, the selection of fiducial markers is not straightforward. For hybrid kV/MV IGRT imaging, larger diameter markers are suggested. If using kV imaging alone, smaller sized markers may be used in smaller sized patients in order to reduce artifacts. This study serves as a guideline for selection of fiducial markers for radiotherapy. However, users are urged to verify the selection of markers and establish clinical protocols optimized for their clinical needs and imaging equipment.

Acknowledgments

The authors would like to thank Dr. Neelam Tyagi for her helpful discussion in this project.

Funding

Maria Chan and Gil'ad Cohen have a research grant with Radiomed Group. However, this work was done outside of that grant and received no funding from any vendor.

Abbreviations

MRI	magnetic resonance imaging
CT	computer tomography
CBCT	cone-beam CT
EPID	electronic portal imaging device
IGRT	image-guided radiotherapy
OBI	on-board imager
kV	kilovoltage
MV	megavoltage
Linac	linear accelerator

References

1. Erickson BJ, Jack CR Jr. Correlation of single photon emission CT with MR image data using fiducial markers. *AJNR Am J Neuroradiol.* 1993; 14(3):713–720. [PubMed: 8517364]
2. Adjamian P, Barnes GR, Hillebrand A, et al. Co-registration of magnetoencephalography with magnetic resonance imaging using bite-bar-based fiducials and surface-matching. *Clin Neurophysiol.* 2004; 115(3):691–698. [PubMed: 15036065]
3. Schiffner DC, Gottschalk AR, Lometti M, et al. Daily electronic portal imaging of implanted gold seed fiducials in patients undergoing radiotherapy after radical prostatectomy. *Int J Radiat Oncol Biol Phys.* 2007; 67(2):610–619. [PubMed: 17236978]
4. Gauthier I, Carrier JF, Beliveau-Nadeau D, Fortin B, Taussky D. Dosimetric impact and theoretical clinical benefits of fiducial markers for dose escalated prostate cancer radiation treatment. *Int J Radiat Oncol Biol Phys.* 2009; 74(4):1128–1133. [PubMed: 19147306]
5. Welsh JS, Berta C, Borzillary S, et al. Fiducial markers implanted during prostate brachytherapy for guiding conformal external beam radiation therapy. *Technol Cancer Res Treat.* 2004; 3(4):359–364. [PubMed: 15270586]
6. Barney BM, Lee RJ, Handrahan D, Welsh KT, Cook JT, Sause WT. Image-guided radiotherapy (IGRT) for prostate cancer comparing kV imaging of fiducial markers with cone beam computed tomography (CBCT). *Int J Radiat Oncol Biol Phys.* 2011; 80(1):301–305. [PubMed: 20864274]
7. van der Wielen GJ, Mutanga TF, Incrocci L, et al. Deformation of prostate and seminal vesicles relative to intraprostatic fiducial markers. *Int J Radiat Oncol Biol Phys.* 2008; 72(5):1604–1611. e3. [PubMed: 19028284]
8. Britton KR, Takai Y, Mitsuya M, Nernoto K, Ogawa Y, Yarmada S. Evaluation of inter- and intrafraction organ motion during intensity modulated radiation therapy (IMRT) for localized prostate cancer measured by a newly developed on-board image-guided system. *Radiat Med.* 2005; 23(1):14–24. [PubMed: 15786747]
9. Killoran JH, Kooy HM, Gladstone DJ, Welte FJ, Beard CJ. A numerical simulation of organ motion and daily setup uncertainties: implications for radiation therapy. *Int J Radiat Oncol Biol Phys.* 1997; 37(1):213–221. [PubMed: 9054898]
10. Huang E, Dong L, Chandra A, et al. Intrafraction prostate motion during IMRT for prostate cancer. *Int J Radiat Oncol Biol Phys.* 2002; 53(2):261–268. [PubMed: 12023128]

11. Skarsgard D, Cadman P, El-Gayed A, et al. Planning target volume margins for prostate radiotherapy using daily electronic portal imaging and implanted fiducial markers. *Radiat Oncol.* 2010; 5:52. [PubMed: 20537161]
12. Khosa R, Nangia S, Chufal KS, Ghosh D, Kaul R, Sharma L. Daily online localization using implanted fiducial markers and its impact on planning target volume for carcinoma prostate. *J Cancer Res Ther.* 2010; 6(2):172–178. [PubMed: 20622364]
13. Yue NJ, Patel AN, Haffty BG, Kim S. Efficacy of fiducial marker-based image-guided radiation therapy in prostate tomotherapy and potential dose coverage improvement using a patient positioning optimization method. *Pract Radiat Oncol.* 2012; 2(2):138–144. [PubMed: 24674089]
14. Kothary N, Dieterich S, Louie JD, Chang DT, Hofmann LV, Sze DY. Percutaneous implantation of fiducial markers for imaging-guided radiation therapy. *Am J Roentgenol.* 2009; 192(4):1090–1096. [PubMed: 19304719]
15. Handsfield LL, Yue NJ, Zhou J, Chen T, Goyal S. Determination of optimal fiducial marker across image-guided radiation therapy (IGRT) modalities: visibility and artifact analysis of gold, carbon, and polymer fiducial markers. *J Applied Clini Med Phys.* 2012; 13(5):3976.
16. Habermehl D, Henkner K, Ecker S, Jakel O, Debus J, Combs SE. Evaluation of different fiducial marker for image-guided radiotherapy and particle therapy. *J Radiat Research.* 2013; 54(suppl 1):i61–i68. [PubMed: 23824129]
17. Jonsson JH, Garpebring A, Karlsson MG, Nyholm T. Internal fiducial markers and susceptibility effects in MRI-simulation and measurement of spatial accuracy. *Int J Radiat Oncol Biol Phys.* 2012; 82(5):1612–1618. [PubMed: 21477942]
18. Hossain M, Schirmer T, Richardson T, Chen L, Buyyounouski MK, Ma CM. Effect of gold marker seeds on magnetic resonance spectroscopy of the prostate. *Int J Radiat Oncol Biol Phys.* 2012; 83(1):451–458. [PubMed: 22245188]
19. Chen Y, O'Connell JJ, Ko CJ, Mayer RR, Belard A, McDonough JE. Fiducial markers in prostate for kV imaging: quantification of visibility and optimization of imaging conditions. *Phys Med Biol.* 2012; 57(1):155–172. [PubMed: 22127351]
20. Zhang M, Kim S, Chen T, Mo X, Haffty BG, Yue NJ. Dose perturbations of gold fiducial markers in the prostate cancer intensity modulated proton radiation therapy (IMPT). *Int J Med Phys Clinic Eng Rad Oncol.* 2012; 1(1):8–13.
21. Huang JY, Newhauser WD, Zhu XR, Lee AK, Kudchadker RJ. Investigation of dose perturbations and radiographic visibility of potential fiducials for proton radiation therapy of the prostate. *Phys Med Biol.* 2011; 56(16):5287–5302. [PubMed: 21799236]
22. Cheung J, Kudchadker RJ, Zhu XR, Lee AK, Newhauser WD. Dose perturbations and image artifacts caused by carbon-coated ceramic and stainless steel fiducials used in proton therapy for prostate cancer. *Phys Med Biol.* 2010; 55(23):7135–7147. [PubMed: 21076190]
23. Huisman HJ, Futterer JJ, Welmers A, et al. Prostate cancer: precision of integrating functional MR imaging with radiation therapy treatment by using fiducial gold markers. *Radiology.* 2005; 236(1):311–317. [PubMed: 15983070]
24. DeLangen M, Hoogeman M, VanderWielen G, DeBoer H, Heijimen B, Levendag P. What is the ultimate fiducial marker? *Radiother Oncol.* 2007; 84:S181–S182.
25. Henry AM, Stratford J, Davies J, et al. An assessment of clinically optimal gold marker length and diameter for pelvis radiotherapy verification using an amorphous silicon flat panel electronic portal imaging device. *Br J Radiol.* 2005; 78(932):737–741. doi:Dx.doi.org/10.1259/bjr/97956788. [PubMed: 16046426]

	MR (3T)	MR (1.5T)	Ultrasound	CT	CBCT	O-Arm	OBI-kV	EPID MV
Solid Au 1.2x3mm (AOS)								
Solid Au 0.8x5mm (AOS)								
VisiCoil 1.1x10mm (IBA)								
VisiCoil .75x10mm (IBA)								
VisiCoil 0.5x10mm (IBA)								
FusionCoil 1x5mm (CIVCO)								
PolyMark 1x3mm (CIVCO)								

Figure 1.
Cropped images of the markers for each imaging modality.

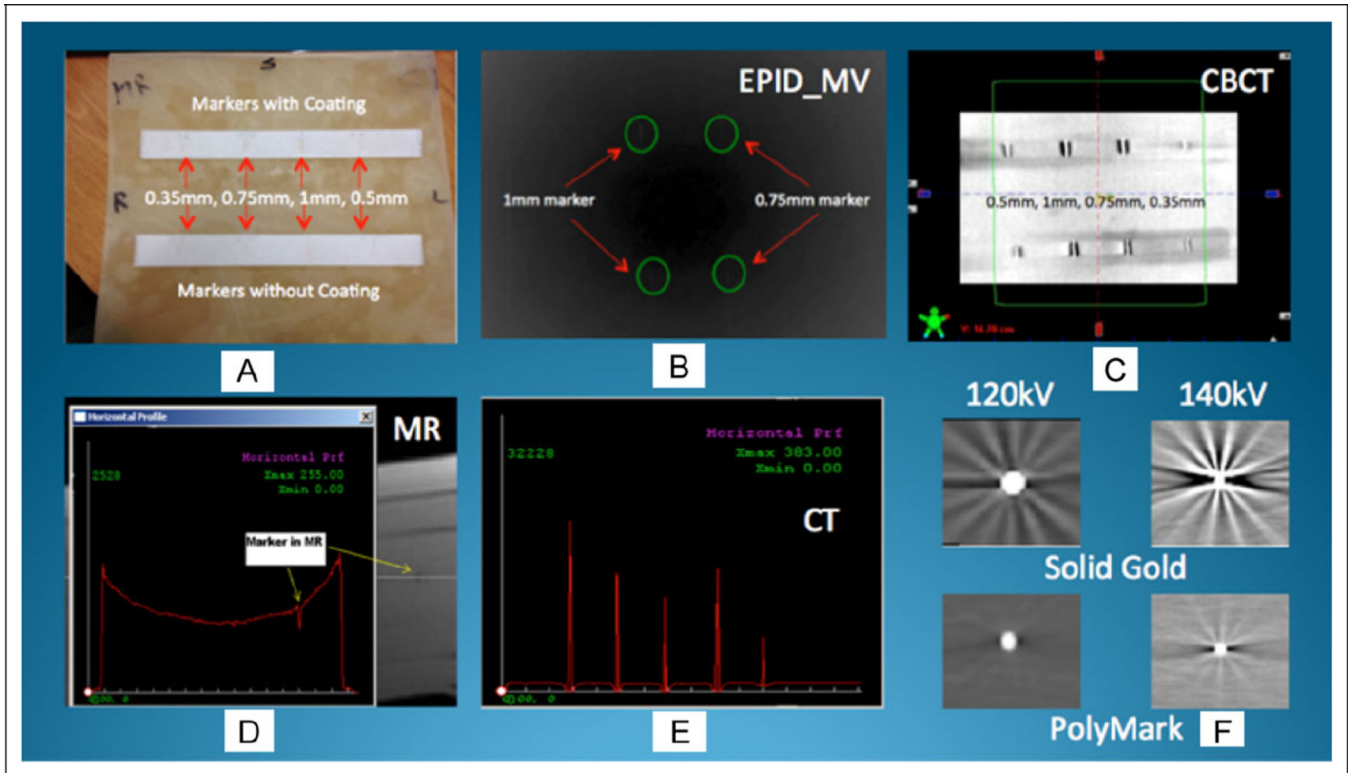


Figure 2.
Imaging and analysis of markers.

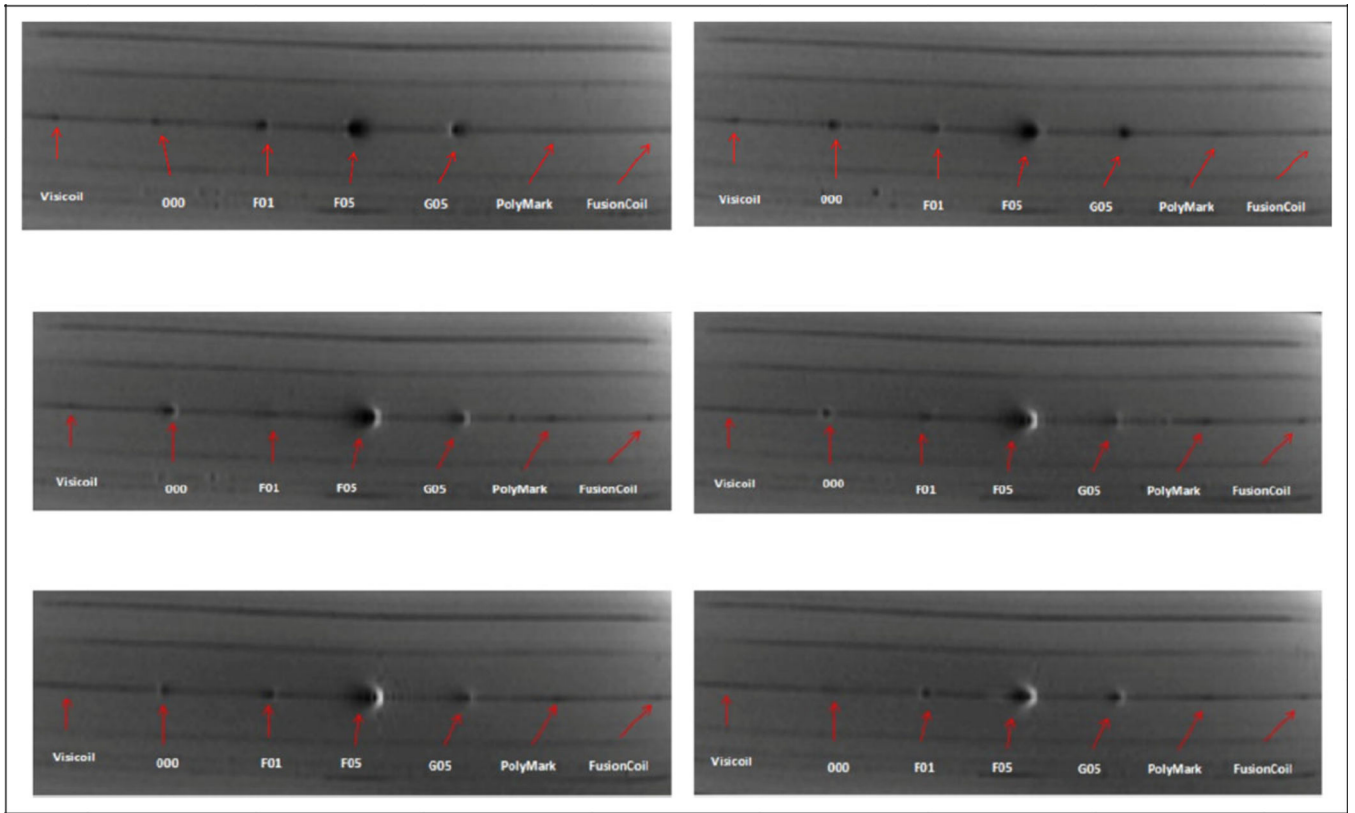


Figure 3.
Axial T1 magnetic resonance (MR) images.

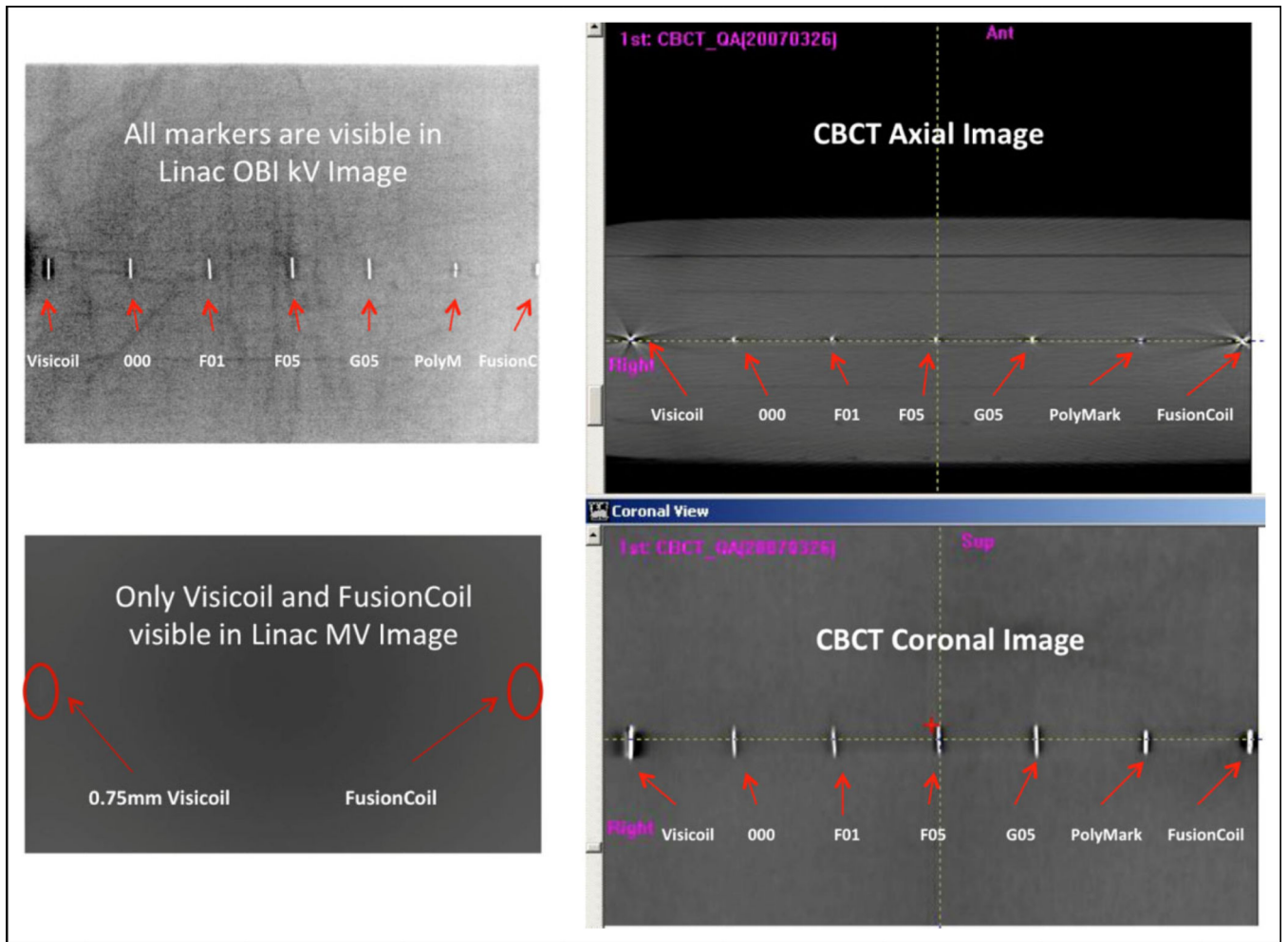


Figure 4. Linear accelerator (Linac)-based kilovoltage (kV), cone-beam computed tomography (CBCT), and megavoltage (MV) images.